JOURNAL OF GUIDANCE, CONTROL, AND DYNAMICS
Vol. 20, No. 5, September–October 1997

Helicopter Attitude Command Attitude Hold Using Individual Channel Analysis and Design

Graham J. W. Dudgeon* and Jeremy J. Gribble†
University of Glasgow, Glasgow G12 8LT, Scotland, United Kingdom

A control law was designed for a linearized model of a typical combat rotorcraft trimmed to 30-kn forward flight. Although based on a single flight condition, the same controller is found, in simulation, to give level 1 performance for the range of speeds from hover to 80 kn, for handling qualities based on small-amplitude motions. Control synthesis was performed using the method of individual channel analysis and design (ICAD). ICAD is a neoclassical, frequency-domain control analysis and design method for multivariable systems. Its most distinctive feature is the use of multivariable structure functions, which make explicit the role of cross coupling in the design process and on the robustness. The control law so obtained is very simple, and the results suggest that modern control methods, based on optimal synthesis, are not a necessity for the helicopter flight control problem.

Nomenclature

G, K	= plant and controller matrices
p, q, r	= body axes angular rates, rad/s
u, v, w	= body axes velocities, ft/s
β_0	= rotor coning angle, rad
β_{1c}	= rotor longitudinal flap angle, rad
β_{1s}	= rotor lateral flap angle, rad
γ_i	= ith multivariable structure function
δ_{coll}	= main rotor collective inceptor
δ_{lat}	= lateral cyclic inceptor
δ_{long}	= longitudinal cyclic inceptor
δ_{tail}	= tail rotor collective inceptor
θ, ϕ, ψ	= Euler angles, rad
θ_0	= main rotor collective blade angle, rad
$\theta_{0_{\text{act}}}$	= main rotor collective actuator state
θ_{0T}	= tail rotor collective blade angle, rad
$\theta_{0T_{\text{act}}}$	= tail rotor collective actuator state
θ_{1c}	= lateral cyclic blade angle, rad
$\theta_{1c_{\text{act}}}$	= lateral cyclic actuator state
θ_{1s}	= longitudinal cyclic blade angle, rad
$\theta_{1s_{\text{act}}}$	= longitudinal cyclic actuator state

I. Introduction

THE publication in 1989 of the revised helicopter handling qualities requirements ADS-33C [now upgraded to ADS-33D (Ref. 1)] has provided a focus for much research into the helicopter flight control problem, by both academic and industrial workers. The highly coupled nature of rotorcraft dynamics has been thought to preclude the use of one-loop-at-a-time control design methods, based on classical single input/single output (SISO) techniques. Hence, much of the research published in the last few years has concentrated on the use of modern control techniques such as eigenstructure assignment,[2,3] $H-\infty$ optimal synthesis,[4,5] and linear quadratic Gaussian optimal synthesis with loop transfer recovery.[6] Methods such as these have the advantage that they can be used to compute all of the SISO elements of a multiloop controller at once. Furthermore, if robustness is assessed within the singular value framework, then statements can be made about the stability robustness of the resulting designs with respect to plant model error. On the other hand, many of the advantages of the classical approach are lost. For example, it is relatively difficult to relate the weighting functions that constitute the design parameters of the various optimal control methods to system performance in a transparent way. Singular values, which are often used to assess system performance and robustness, are abstract mathematical concepts that may be difficult to interpret physically. Finally, the resulting control laws are usually of relatively high order in contrast to classically designed controllers (for SISO plants), which are no more complicated than they need to be in order to meet the specifications.

This paper is concerned with the application of individual channel analysis and design (ICAD)[7–10] to a model of a typical combat helicopter[11] to obtain multivariable control laws that meet the specifications contained within ADS-33D (Ref. 1). ICAD is a frequency-domain-based framework for the analysis and design of multivariable control laws. Its main feature is the use of multivariable structure functions (MSFs), which explicitly characterize the inherent system multivariable structure due to the loop interaction. These MSFs quantify whether the loop interaction is small or large and, if large, whether it is benign or malign. The MSFs are used for design purposes and also to supplement the channel stability margins, obtained by breaking one loop at a time, to provide a framework for analyzing stability robustness in a transparent way that takes into account the effects of loop interaction. Because the synthesis of individual diagonal elements of the feedback control matrix is performed using classical SISO techniques, these elements are of relatively low order and are no more complicated than necessary, making controllers of this type eminently suitable for gain scheduling.

Previous studies of the helicopter flight control problem using the ICAD method[10] addressed the problem of designing for good handling qualities in only a preliminary fashion, and the outputs that were controlled did not form a recognized response type. In the following sections of the paper, the relevant performance specifications from ADS-33D (Ref. 1) are summarized and a description of the ICAD method for four input/four output systems is presented. ICAD is then specifically applied to the design of an attitude command attitude hold (ACAH) system and the small-signal handling qualities are assessed.

II. Handling Qualities

Handling qualities specifications, as stated in ADS-33D (Ref. 1), are categorized in terms of response types from which flying qualities levels can be assessed. The response types are dependent on specific mission task elements (MTEs), such as target acquisition and tracking, which requires ACAH response when the helicopter is in a degraded visual cue environment. Other response types include rate command direction hold, which is necessary in a degraded visual cue environment for an MTE, such as slope landing and translational rate command, which is necessary for a task such as precision hover, in a severely degraded visual cue environment.

Received Jan. 26, 1996; revision received May 12, 1997; accepted for publication May 22, 1997. Copyright © 1997 by the American Institute of Aeronautics and Astronautics, Inc. All rights reserved.

*Ph.D. Student, Department of Electronics and Electrical Engineering; currently Higher Scientific Officer/Research Worker, Rotorcraft Group, Flight Management and Control Department, Defence Evaluation and Research Agency, Bedford MK41 6AE, England, UK.

†Lecturer, Centre for Systems and Control, Department of Electronics and Electrical Engineering.

Flying qualities levels are derived from the Cooper–Harper pilot ratings (CHPR) scale and are defined in Table 1. The handling qualities specifications are defined in both the time domain and the frequency domain when considering small-amplitude signals. The frequency-domain specifications relate to the response the pilot sees, i.e., the closed-loop augmented helicopter if automatic control is implemented, or the unaugmented helicopter if no automatic control is implemented, and ensures that the pilot has sufficient bandwidth and acceptable phase delay between commanded response and actual response. Two bandwidths are defined in ADS-33D (Ref. 1): the phase-limited bandwidth $\omega_{\mathrm{BW}_{\mathrm{phase}}}$ and the gain-limited bandwidth $\omega_{\mathrm{BW}_{\mathrm{gain}}}$ (Fig. 1). The $\omega_{\mathrm{BW}_{\mathrm{phase}}}$ is the frequency at which the response the pilot sees has a phase of -135 deg. The $\omega_{\mathrm{BW}_{\mathrm{gain}}}$ is the frequency at which the gain of the response the pilot sees is 6 dB greater than the gain at $\omega_{-180\,\mathrm{deg}}$. When the response type is ACAH it is recommended that $\omega_{\mathrm{BW}_{\mathrm{phase}}}$ is less than $\omega_{\mathrm{BW}_{\mathrm{gain}}}$ to ensure that at least 6 dB of gain margin is available to the pilot. This 6-dB gain margin helps minimize the risk of pilot-induced oscillations when the pilot is either performing a precision task or is maneuvering the helicopter aggressively.

The phase delay of a response is calculated as

$$\tau_p = \frac{\Delta\Phi 2\omega_{-180\,\mathrm{deg}}}{57.3(2\omega_{-180\,\mathrm{deg}})} \tag{1}$$

where $\Delta\Phi 2\omega_{-180\,\mathrm{deg}}$ is the phase difference between -180 deg and the phase at $2\omega_{-180\,\mathrm{deg}}$. The phase delay parameters and the handling qualities bandwidths are shown in diagrammatic form in Fig. 1. The time-domain requirements specify bounds on cross coupling, damping, and in the case of height rate the shape of response.

A 30-kn forward flight condition is considered, and so the handling qualities requirements for hover and low speed (speeds less than 45 kn) should be addressed. Table 2 shows the small-signal requirements for the hover and low-speed regime. Also shown in Table 2 are the outputs to which the requirements relate and whether the analysis is performed in the time domain or the frequency domain.

Table 1 Definition of handling qualities levels

Level 1, CHPR 1–3.5	MTE can be completed with minimal pilot compensation. Satisfactory without improvement.
Level 2, CHPR 3.5–6.5	MTE can be completed but requires moderate/considerable pilot compensation. Deficiencies warrant improvement.
Level 3, CHPR 6.5–8.5	Considerable pilot compensation required to maintain control of rotorcraft. Deficiencies require improvement.

III. Individual Channel Analysis

The helicopter under consideration is a typical combat rotorcraft trimmed at 30-kn forward flight and has four inputs and four outputs. This section describes individual channel analysis (ICA) for specific use with a system of this size. For a more general description the reader is referred to Ref. 8. A 4×4 diagonal control matrix K is placed in the forward path immediately before the 4×4 plant matrix G and a feedback loop is closed around GK. An individual channel (channel for brevity) is formed by opening the loop between one input–output pairing and leaving the remaining three loops closed. The motivation behind doing this is that the resulting transfer function is SISO, and so classical SISO techniques can be applied, but with the benefit that the effects of cross coupling are included in full. Figure 2 shows a block diagram of the ICAD configuration for analysis of the height rate response.

To derive the transfer function for a particular channel, the transfer function matrix G must be appropriately partitioned (as is seen in Fig. 2). Focusing on the height rate response, G is partitioned as

$$G = \begin{bmatrix} g_{11} & G_{12} \\ G_{21} & G_{22} \end{bmatrix} \tag{2}$$

Table 2 ADS-33D (Ref. 1) small-signal requirements for hover and low speed

Section	Title	Output(s)	Domain
3.3.2	Small amplitude pitch (roll) attitude changes	θ, ϕ	Frequency Time
3.3.5	Small amplitude yaw attitude changes	ψ	Frequency Time
3.3.9	Interaxis coupling	$\dot{h}, \theta, \phi, r$	Time
3.3.9.1	Yaw due to collective	$\dot{h}, r$	Time
3.3.9.2	Pitch to roll (roll to pitch)	θ, ϕ	Time
3.3.10	Response to collective controller	$\dot{h}$	Time
3.3.10.1	Height response characteristics	$\dot{h}$	Time

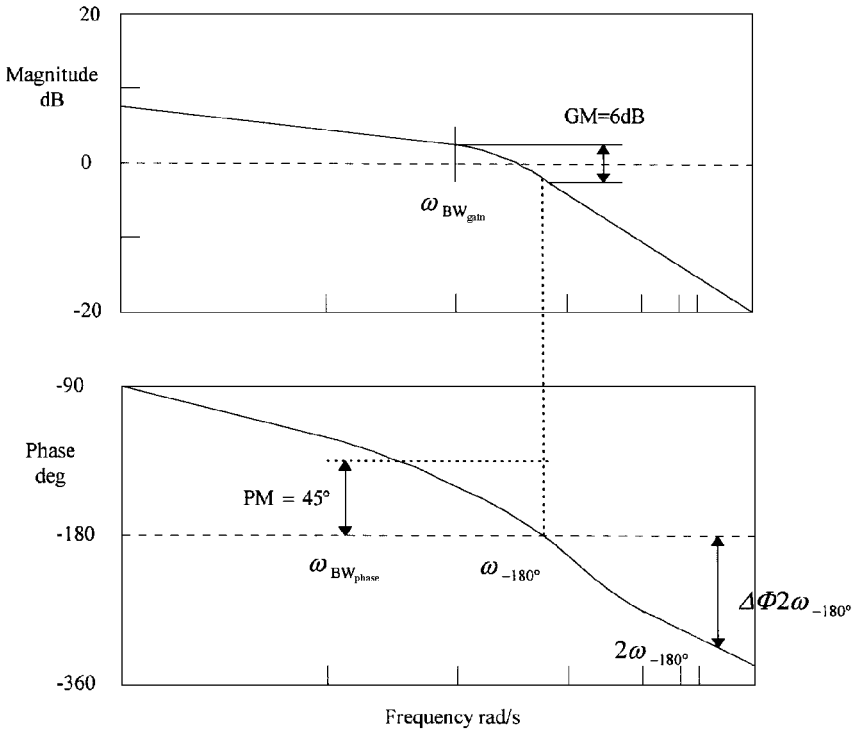

Fig. 1 Definitions of bandwidth and phase delay.

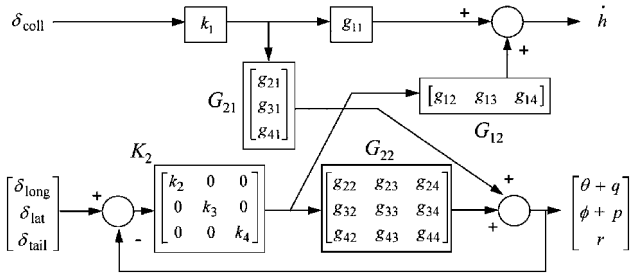

Fig. 2 Block diagram for determination of channel 1.

The height rate response to input δ_{coll} is given by

$$C_1 = k_1 g_{11}(1 - \gamma_1) \tag{3}$$

where γ_1 is defined as

$$\gamma_1 = -\frac{|\bar{G}_1|}{g_{11}|\bar{G}^1|} \tag{4}$$

and where $\bar{G} = K^{-1} + G$. $\bar{G}_1$ is $\bar{G}$ with element (1, 1) set to zero; $\bar{G}^1$ is $\bar{G}$ with row 1 and column 1 removed. Here, $|\ |$ is the determinant. The diagonal elements of $\bar{G}$ are $(k_i^{-1} + g_{ii})$, $i = 1, \ldots, 4$, which can be rewritten as g_{ii}/h_i, where $h_i = k_i g_{ii}/(1 + k_i g_{ii})$ is the ith closed-loop subsystem obtained when only the ith loop is closed. Note that γ_1 is known as the MSF of the height rate channel.

C_1 is the height rate channel and is the transfer function that describes the dynamics of the height rate due to a command on its primary input, the main rotor collective inceptor δ_{coll}, when the height rate loop is open but the other three loops are closed. The effect of δ_{long}, δ_{lat}, and δ_{tail} on $\dot{h}$ can be considered as an additive disturbance at the output of channel 1.

This procedure can also be applied to the other three input–output pairings, hence forming four channels in total, given as

$$C_i = k_i g_{ii}(1 - \gamma_i), \qquad i = 1, \ldots, 4 \tag{5}$$

where C_1 is $\dot{h}$ due to δ_{coll}, C_2 is $\theta + q$ due to δ_{long}, C_3 is $\phi + p$ due to δ_{lat}, and C_4 is r due to δ_{tail}.

Next, γ_i is given as

$$\gamma_i = -\frac{|\bar{G}_i|}{g_{ii}|\bar{G}^i|} \tag{6}$$

where $\bar{G}_i$ is $\bar{G}$ with element (i, i) set to zero. $\bar{G}^i$ is $\bar{G}$ with row i and column i removed. The frequency response of channel C_i, $i = 1, \ldots, 4$, can be used to analyze the transient response and reference tracking of the ith output due to the ith input, for the nominal system, in exactly the same way as in a classical single-loop system.

ICAD recognizes that the $\gamma_i, i = 1, \ldots, 4$, have implications for the stability robustness of the closed-loop system. Referring to Eq. (5), if the Nyquist plot of γ_i is close to the (1, 0) point, then a sensitivity problem may exist. There are two types of sensitivity that can arise due to γ_i approaching the (1, 0) point. These are structural sensitivity and phase sensitivity. Structural sensitivity occurs when γ_i is close enough to the (1, 0) point such that plant variation may cause it to traverse the (1, 0) point. By consideration of the Nyquist criterion, this means that the zero structure of $(1 - \gamma_i)$ will change, hence changing the zero structure of C_i. If a right-hand plane zero (RHPZ) is introduced into C_i at a frequency where there is sufficient loop gain for a pole of $C_i/(1 + C_i)$ to be attracted to it and move into the right-hand plane (RHP), then the system will become unstable. Structural sensitivity is problematic at frequencies where the channel loop gain is greater than one, i.e., at frequencies below crossover. Phase sensitivity is the situation where large variations in phase can occur in a channel due to only small changes in the plant. If γ_i is close to (1, 0) near the 0-dB crossover frequency of channel i, then small changes in the plant can give rise to very large changes in the phase of the channel frequency response, with the possibility that the channel encirclement count of the $(-1, 0)$ point will change, causing instability even if the channel phase margins are generous according to the usual criteria. In summary, a closed-loop system may be regarded as being stability robust if the C_i have adequate gain and phase margins and the γ_i are far from the (1, 0) point at frequencies of importance (at and below channel crossover frequencies).

Before the controllers have been designed one can use the constrained variable method,[12] that is, to assume that the controllers have infinite gain, in order to determine potential stability robustness problems. Approximate channel MSFs can be defined to this end. They are given as

$$\hat{\Gamma}_i = -\frac{|G_i|}{g_{ii}|G^i|}, \qquad i = 1, \ldots, 4 \tag{7}$$

where G_i is G with element (i, i) set to zero and G^i is G with row i and column i removed. If any of the $\hat{\Gamma}_i$ are close to the $(+1, 0)$ point at frequencies of importance, then there is a potential stability robustness problem.

IV. Controller Design Using ICA

The design procedure involves relating the transmission zeros of the helicopter, which are the zeros of $|G|$, to the poles of the closed-loop system, which are the zeros of $|I + GK|$. The design of the diagonal control law can proceed using a nested technique. Full details of this technique are given in Ref. 7.

For a four input/four output system, $|G|$ can be expanded as[7]

$$|G| = (1 - \Gamma_1)g_{11}(1 - \Gamma_2)g_{22}(1 - \Gamma_3)g_{33}g_{44} \tag{8}$$

where

$$\Gamma_i = -\frac{\left|G_i^{1,\ldots,(i-1)}\right|}{g_{ii}|G^{1,\ldots,i}|}, \qquad i = 1, \ldots, 4 \tag{9}$$

$G_i^{1,\ldots,(i-1)}$ is G with element (i, i) set to zero and rows and columns $1, \ldots, (i-1)$ removed. $G^{1,\ldots,i}$ is G with rows and columns $1, \ldots, i$ removed. The Γ_i are known as nested approximate MSFs. Notice that, by definition, Γ_4 is equal to zero for a four input/four output system.

Define

$$|I + GK| = |\hat{G}| \tag{10}$$

$|\hat{G}|$ can be expanded as[7]

$$|\hat{G}| = [1 + k_1 g_{11}(1 - \gamma_1)] \cdot [1 + k_2 g_{22}(1 - \gamma_{12})] \times [1 + k_3 g_{33}(1 - \gamma_{123})] \cdot [1 + k_4 g_{44}] \tag{11}$$

Define

$$C_1' = k_i g_{ii}(1 - \gamma_{1,\ldots,i}), \qquad i = 1, \ldots, 4 \tag{12}$$

The C_i' are known as nested channels. Also,

$$\gamma_{1,\ldots,i} = -\frac{\left|\bar{G}_i^{1,\ldots,(i-1)}\right|}{g_{ii}|\bar{G}^{1,\ldots,i}|}, \qquad i = 1, \ldots, 4 \tag{13}$$

$\bar{G}_i^{1,\ldots,(i-1)}$ is $\bar{G}$ with element (i, i) set to zero and rows and columns $1, \ldots, (i-1)$ removed. $\bar{G}^{1,\ldots,i}$ is $\bar{G}$ with rows and columns $1, \ldots, i$ removed. The $\gamma_{1,\ldots,i}$ are known as nested actual MSFs. Notice that by definition γ_{1234} is equal to zero for a four input/four output system.

The ICA approach allows one to assess from the MSFs the conditions under which it is possible to stabilize the plant using a diagonal controller. In particular the following result, specialized to our immediate requirements, can be proved.[7]

To stabilize an m-input/m-output minimum-phase plant whose MSFs have a high-frequency limit of less than one, it is sufficient that the $\gamma_{1,\ldots,j}$, $j = 1, \ldots, (m-1)$, have the same pole structure and encirclement count as the Γ_j and that the number of RHPZs of the $(1 + C_i')$, $i = 1, \ldots, m$, are the same as the number of RHPZs of the C_i'. This condition will be used later in Sec. VII.

V. Design Considerations

The first requirement of the design is that it is an ACAH system, i.e., a commanded input in δ_{long} or δ_{lat} will yield a proportional pitch or roll attitude, respectively, and, in addition, the system must regulate the pitch and roll attitudes to their trim values when there are no commanded inputs.

Because angular rate signals are available to the system, it is desirable to feed back a blend of the appropriate rates with the attitudes in order to provide phase lead at low-noise levels to the feedback system. By using a blend of this type, the phase lead requirements of the controller will be reduced. In addition to providing phase lead, the stability derivatives M_q and L_p will be augmented by feeding back the pitch and roll rates, respectively. This provides additional damping of the pitch and roll responses. In straight and level flight,

$$q \approx \dot{\theta} \tag{14}$$

$$p \approx \dot{\phi} \tag{15}$$

Taking the pitch attitude as an example, if one were to produce a linear blend of the pitch attitude and pitch rate of the form

$$\theta + kq \approx \theta(1 + ks) \tag{16}$$

then it is seen that a stable zero has effectively been introduced to the θ response at k^{-1} rad/s.

As the required 0-dB crossovers are envisaged to be above 1 rad/s, k will be set to one for both the pitch and roll responses, hence introducing an effective zero at 1 rad/s in each of the attitude channels. This will provide appropriate phase lead at the frequencies of interest for design, without compromising the ability of the system to track and regulate the attitudes below 1 rad/s.

It is possible to determine approximately the phase-limited bandwidth from the open-loop channel frequency response. To do this, three values are required. These are 1) the 0-dB crossover frequency $\omega_{0\text{dB}}$ of the open-loop channel, 2) the associated phase margin, and 3) the -180-deg crossover frequency $\omega_{-180\,\text{deg}}$. The phase of the closed-loop channel i at $\omega_{0\text{dB}}$ can be calculated from values 1 and 2 by the following equation:

$$\varphi_{\text{CL}i} = \angle\left(\frac{-e^{j\eta_i}}{1 - e^{j\eta_i}}\right) \tag{17}$$

where $\varphi_{\text{CL}i}$ is the closed-loop phase of channel i at $\omega_{0\text{dB}}$, $\angle$ is the angle, and η_i is the phase margin of channel i. The -180-deg crossover frequency of channel i $\omega_{-180\,\text{deg}}$ will be the same as the closed loop channel i -180-deg crossover frequency. This is because $C_i(j\omega_{-180\,\text{deg}})$ is a negative real number whose magnitude is less than one, and so the closed loop, $C_i(j\omega_{-180\,\text{deg}})/[1 + C_i(j\omega_{-180\,\text{deg}})]$, will also be a negative real number. If it is assumed that the closed-loop phase decrease between $\omega_{0\text{dB}}$ and $\omega_{-180\,\text{deg}}$ is linear on the logarithmic scale, then an approximation of the phase-limited bandwidth can be made. Therefore, specifications for the open-loop channels should include not only a designated 0-dB crossover frequency and phase margin, but also a -180-deg crossover frequency, the values being set to achieve a required phase-limited bandwidth.

Because it is the bandwidth of the θ, ϕ, and ψ responses, rather than $\theta + q$, $\phi + p$, and r, which is of interest, appropriate amendments must be made to the approximate closed-loop phase plots generated by consideration of the chosen feedback signals. The θ and ϕ responses are effectively the $\theta + q$ and $\phi + p$ responses but each with an additional stable pole at 1 rad/s. The ψ response is effectively the r response but with a pole at the origin. The phase response of the effective pole can be superimposed on the approximate closed-loop phase plots of the $\theta + q$, $\phi + p$, and r and superposition used to calculate the approximate phase behavior of the θ, ϕ, and ψ responses. The handling qualities phase-limited bandwidth is defined as being the frequency at which the closed-loop attitude phase responses are -135 deg. Because the -135-deg phase of the approximate θ, ϕ, and ψ responses may not be within the frequency range between $\omega_{0\text{dB}}$ and $\omega_{-180\,\text{deg}}$ of the approximate $\theta + q$, $\phi + p$, and r responses, due to the phase decrease introduced by the effective poles, it is sufficient to extrapolate the response to the frequency at which the phase is -135 deg, $\omega_{-135\,\text{deg}}$. In most cases $\omega_{-135\,\text{deg}}$ will be close enough to $\omega_{0\text{dB}}$ such that linear extrapolation is locally valid. As a rule of thumb, if one designs the $\theta + q$ and $\phi + p$ channels to have gain margins of at least 10 dB, then the phase-limited bandwidths are likely to be less than the gain-limited bandwidths, which is preferred for an ACAH system.

Table 3 Approximate open-loop channel specifications

	$\omega_{0\text{dB}}$, rad/s	$\omega_{-180\,\text{deg}}$, rad/s	$\omega_{\text{BW}_{\text{phase}}}$, rad/s	PM,[a] deg	GM,[b] dB
Channel 1	1.0	×	n/a	55.0	20.0
Channel 2	3.0	10.0	2.9	50.0	10.0
Channel 3	3.2	13.0	3.1	50.0	10.0
Channel 4	5.0	20.0	4.0	55.0	20.0

[a]Phase margin. [b]Gain margin.

Table 4 Structure of $G(s)$

	RHP transmission zeros, rad/s	RHP eigenvalues, rad/s
$G(s)$	——	$9.1439e{-}2 \pm 4.6032e{-}1j$

Table 5 Structure of parameters of Eq. (8)

	RHPZs, rad/s	RHPPs, rad/s
$\lvert G\rvert$	——	$9.1439e{-}2 \pm 4.6032e{-}1j$
$(1 - \Gamma_1)$	$9.1439e{-}2 \pm 4.6032e{-}1j$	$9.2078e{-}2 \pm 3.9896e{-}1j$
$(1 - \Gamma_2)$	$9.1439e{-}2 \pm 4.6032e{-}1j$	$3.9534e{-}2 \pm 4.0786e{-}1j$
		$1.9633e{-}2$
$(1 - \Gamma_3)$	$9.1439e{-}2 \pm 4.6032e{-}1j$	$1.1838e{-}1 \pm 4.9502e{-}1j$
	$3.9534e{-}2 \pm 4.0786e{-}1j$	$8.7159e{-}2 \pm 3.7749e{-}1j$
g_{11}	$9.2078e{-}2 \pm 3.9896e{-}1j$	$9.1439e{-}2 \pm 4.6032e{-}1j$
g_{22}	$1.9633e{-}2$	$9.1439e{-}2 \pm 4.6032e{-}1j$
g_{33}	$1.1838e{-}1 \pm 4.9502e{-}1j$	$9.1439e{-}2 \pm 4.6032e{-}1j$
g_{44}	$8.7159e{-}2 \pm 3.7749e{-}1j$	$9.1439e{-}2 \pm 4.6032e{-}1j$

Table 3 shows the open-loop specifications for the design with the approximate handling qualities parameters. The × on the channel 1 specification for $\omega_{-180\,\text{deg}}$ means that it can be placed arbitrarily as there is no handling qualities bandwidth requirement for the height rate response. These specifications are for guidance only, and there is no requirement on the designer to meet them exactly or to interpret them as being lower limits that must be met. It is usually sufficient that the appropriate parameters of the final design are within some close vicinity of the open-loop specifications. How close is subjective and is left to the designer's judgement. In the event that the first iteration of the design does not meet the handling qualities requirements, it is likely that the number of further iterations required will be substantially reduced, as opposed to a design where no consideration of the approximate handling qualities parameters have been made.

VI. Approximate Sensitivity Analysis of ACAH System

The helicopter model is a 19th-order state-space representation of a typical combat rotorcraft trimmed at 30-kn forward flight. The model has nine rigid body states, six rotor states, and four actuator states. The state-space model is given in the Appendix. The helicopter is given in transfer function form by

$$G(s) = C(sI - A)^{-1}B \tag{18}$$

Table 4 shows the structure of the RHP transmission zeros and eigenvalues of the system. [In the classical control theory of SISO systems, the number and location of the right-hand plane poles (RHPPs) and zeros play an important role in determining the potential stability, performance, and robustness, but the number and location of the left-hand plane poles and zeros are much less crucial. These ideas generalize to multivariable systems: in particular, it is the RHPPs and zeros that are of interest and, for brevity, only these are shown in Tables 4 and 5.]

The sensitivity analysis involves inspecting the approximate channel MSFs. Figure 3 shows the Nyquist plot of $\hat{\Gamma}_3$, the approx-

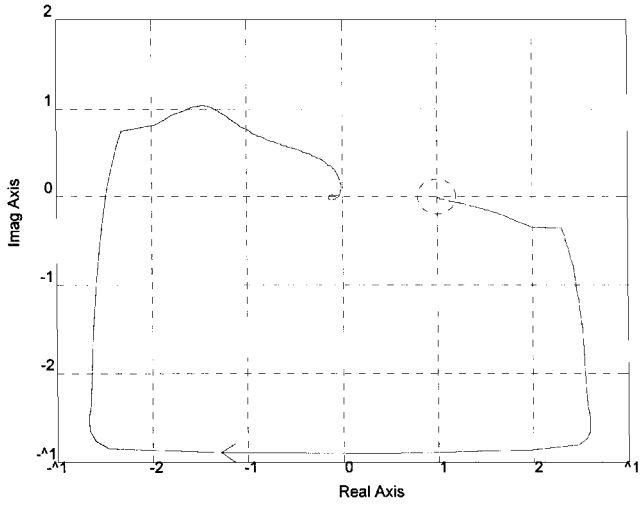

Fig. 3 Nyquist plot of $\hat{\Gamma}_3$.

imate MSF of channel 3, i.e., the $\phi + p$ channel. Note that the axis scaling is linear between ± 2 but logarithmic otherwise. It is seen that $\hat{\Gamma}_3$ approaches the $(1, 0)$ point quite closely at low frequencies, below about 0.1 rad/s. The other approximate MSFs were found to closely approach the $(1, 0)$ point at frequencies not exceeding 0.1 rad/s and were adequately far from the $(1, 0)$ point at other frequencies.

It can be concluded from this sensitivity analysis that the actual system will exhibit potential sensitivity only at low frequencies if high-performance control is used.

VII. Design of ACAH Control Law

From Sec. V it was determined that the 0-dB crossover frequencies of the channels should be 1, 3, 3.2, and 5 rad/s, respectively. For systems whose channels are defined to have different bandwidths, the most appropriate numbering of the channels is such that the lowest bandwidth channel is defined as channel 1 and the highest bandwidth channel is defined as channel 4. It turns out that the requirements of the system naturally impose numbering on the channels, which is compatible with this philosophy.

The physical interpretation of the nested channels of Eq. (11) are given as follows.

1) C_1' is the transfer function describing $\dot{h}$ due to δ_{coll} when the height rate is open but the $\theta + q$, $\phi + p$ and yaw rate loops are closed.

2) C_2' is the transfer function describing $\theta + q$ due to δ_{long} when the height rate loop and $\theta + q$ loops are open but the $\theta + p$ and the yaw rate loops are closed.

3) C_3' is the transfer function describing $\phi + p$ due to δ_{lat} when the height rate, $\theta + q$, and $\phi + p$ loops are open but the yaw rate loop is closed.

4) C_4' is the transfer function describing r due to δ_{tail} when all of the feedback loops are open.

Before the controllers have been designed, one uses Eq. (8) to assess the potential achievable performance. Γ_1, Γ_2, and Γ_3 are written explicitly as

$$\Gamma_1 = -\begin{vmatrix} 0 & g_{12} & g_{13} & g_{14} \\ g_{21} & g_{22} & g_{23} & g_{24} \\ g_{31} & g_{32} & g_{33} & g_{34} \\ g_{41} & g_{42} & g_{43} & g_{44} \end{vmatrix} \Bigg/ g_{11} \begin{vmatrix} g_{22} & g_{23} & g_{24} \\ g_{32} & g_{33} & g_{34} \\ g_{42} & g_{43} & g_{44} \end{vmatrix} \tag{19a}$$

$$\Gamma_2 = -\begin{vmatrix} 0 & g_{23} & g_{24} \\ g_{32} & g_{33} & g_{34} \\ g_{42} & g_{43} & g_{44} \end{vmatrix} \Bigg/ g_{22} \begin{vmatrix} g_{33} & g_{34} \\ g_{43} & g_{44} \end{vmatrix} \tag{19b}$$

$$\Gamma_3 = \frac{g_{34}g_{43}}{g_{33}g_{44}} \tag{19c}$$

Figure 4 shows the Nyquist plots of Γ_1, Γ_2, and Γ_3. Highlighted in Fig. 4 is the position of the MSFs at 1 rad/s. It is seen that the magnitude of the MSFs above 1 rad/s is small, hence loop interaction is small, and so designing the 0-dB crossovers of the channels at the frequencies specified in Table 1 will not pose any difficulties. Table 5 shows the structures of the parameters of Eq. (8). The nested nature of the Γ_j, $j = 1, \ldots, 3$, is evident. Notice that the zeros of the $(1 - \Gamma_j)$ contain RHPZs that exactly correspond to the eigenvalues of the system and so can be disregarded in the structural assessment. Details of this phenomenon are described in more detail in Ref. 9.

The expansion of the $(1, 0)$ region in Fig. 4 is to enable the reader to clearly see the number of encirclements of the $(1, 0)$ point of Γ_2 and Γ_3. From Table 5 it is seen that g_{33}, g_{44}, and $(1 - \Gamma_3)$ have noncanceling RHPZs, and this tells us that potentially the helicopter cannot be stabilized by high-performance control of the lateral system only. This makes sense as the unstable poles of the system can be interpreted as being an unstable phugoid mode and, hence, originate in the longitudinal dynamics. High-performance lateral control will, therefore, be unable to stabilize this mode. However, closure of loops 2–4 will potentially stabilize the plant, as will closure of all four loops. To show this, we refer to the condition stated at the end of Sec. IV.

If one designs high-performance control, then at frequencies below the desired 0-dB crossovers the $\gamma_{1,\ldots,i}$ can be made arbitrarily close to the Γ_i in the low- to mid-frequency range. Also, the controllers will be designed such that the $(1 + C_i')$ have the same number of RHPZs as the C_i'. All that remains is to check that the encirclements of the $(1, 0)$ point of the $\gamma_{1,\ldots,i}$ at high frequency are the same as that of the Γ_i. Figure 4 shows the value of the Γ_i at 1 rad/s. It is seen that the high-frequency regions of the Γ_i are quite close to the origin. Because the $\gamma_{1,\ldots,i}$ will be arbitrarily close to the Γ_i in the low- to mid-frequency region and then attenuate to the origin in the high-frequency region, the number of encirclement counts of the $\gamma_{1,\ldots,i}$ will be the same as the Γ_i.

The design should start with controller k_4 and end with controller k_1. At each stage it is sufficient to place the 0-dB crossovers of the nested channels at the desired 0-dB crossovers of the actual channels. This gives a good first try for the controllers. Once the first iteration of design is complete, the design can be fine tuned if desired.

Note that the described method is different from sequential loop closure,[13] as stability of the system after each loop closure is not required. Closed-loop stability is only required after all four loops are closed.

The controllers were designed, using classical loop shaping techniques, to give channel crossover frequencies and stability margins close to those specified in Table 3, together with good behavior in the crossover region. Integral or near-integral action was introduced, giving high channel magnitudes at low frequencies, to eliminate the steady-state tracking error and off-axis coupling. An extra high-frequency pole was introduced into each controller, increasing the high-frequency rolloff, to reduce the impact of sensor noise and high-frequency unmodeled dynamics and also to meet the specifications on $\omega_{-180\,\text{deg}}$ given in Table 3. The controller transfer functions were

$$k_1 = \frac{0.13(s+1)}{s(s+10)} \tag{20}$$

$$k_2 = \frac{0.45(s+1)(s+1.1)(s+2)}{s(s+0.001)(s+3.4)(s+40)} \tag{21}$$

$$k_3 = -\frac{0.3(s+1)(s+4.2)}{s(s+0.001)(s+90)} \tag{22}$$

$$k_4 = -\frac{0.7(s+2)}{s(s+25)} \tag{23}$$

It was found necessary to implement a decoupling filter outside the feedback system to reduce the yaw rate due to collective. This filter was placed between the height rate and yaw rate inputs. A shaping filter for the height rate was also necessary after implementation of the decoupler. The decoupling filter is given as

$$d_{\text{yaw\_coll}} = -\frac{4s}{(s+3)(s+6)} \tag{24}$$

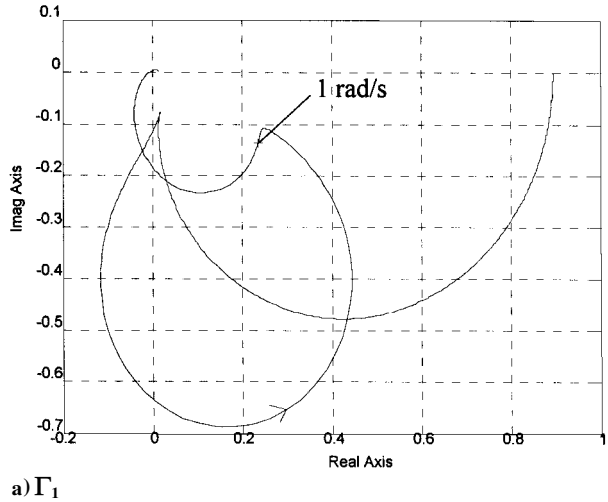

a) Γ_1

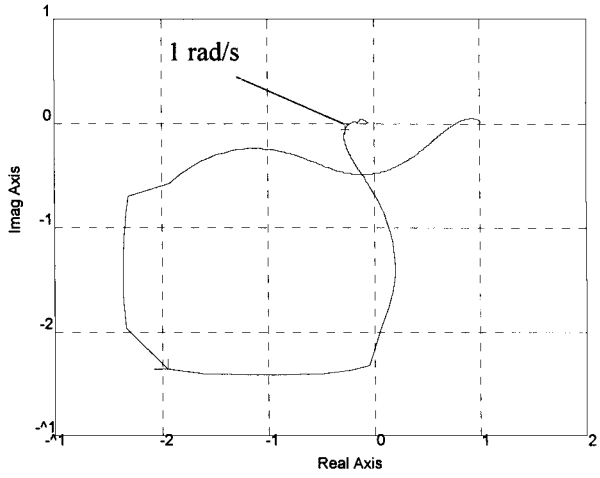

b) Γ_2

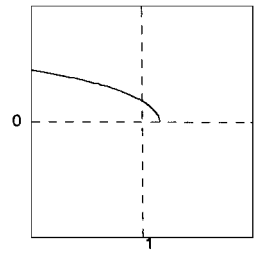

b′) Expansion of (1, 0) region of Γ_2

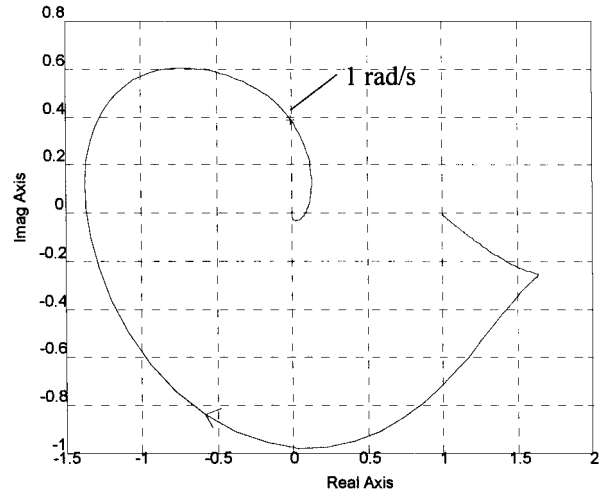

c) Γ_3

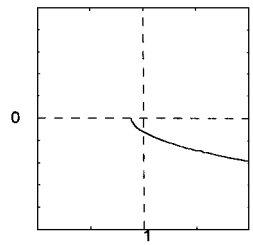

c′) Expansion of (1, 0) region of Γ_3

Fig. 4 Nyquist plot.

and the shaper is given as

$$s_h = \frac{7.14(s+0.7)}{(s+0.5)(s+10)} \tag{25}$$

VIII. ICA of ACAH System

Figure 5 shows the Bode plot of the $\phi + p$ channel, and it is seen to be good by classical design criteria, i.e., high gain at frequencies below crossover, smooth slope over the 0-dB region, and adequate attenuation of gain in the high-frequency region. Notice that the attenuation of the gain after 0-dB crossover is not as steep as it could be between 3 and 10 rad/s, although it is by no means inadequate. This is a consequence of requiring additional phase lead at frequencies beyond the 0-dB crossover frequency to meet the level 1 phase delay requirements of the roll attitude response. In this case, the decrease in attenuation is regarded as being an acceptable tradeoff to achieve level 1 requirements.

Table 6 shows the phase and gain margins, crossover frequencies, and handling qualities bandwidths of the actual channels. It is seen that all gain and phase margins are adequate. However, the channel

Table 6 Channel parameters of final design

	ω_{0dB}, rad/s	$\omega_{-180\,deg}$, rad/s	$\omega_{BW_{phase}}$, rad/s	PM,[a] deg	GM,[b] dB
Channel 1	0.99	n/a	n/a	66.03	28.68
Channel 2	2.73	10.40	2.70	47.74	13.36
Channel 3	3.11	13.90	3.06	51.98	10.37
Channel 4	4.58	23.70	3.62	54.24	20.36

[a]Phase margin. [b]Gain margin.

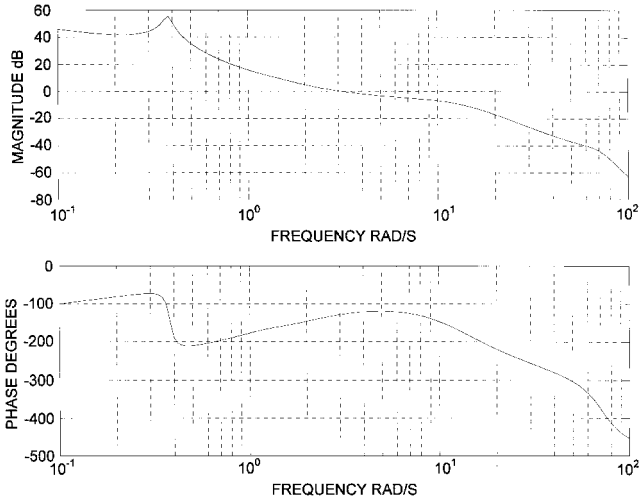

Fig. 5 Bode plot of open-loop $\phi + p$ channel.

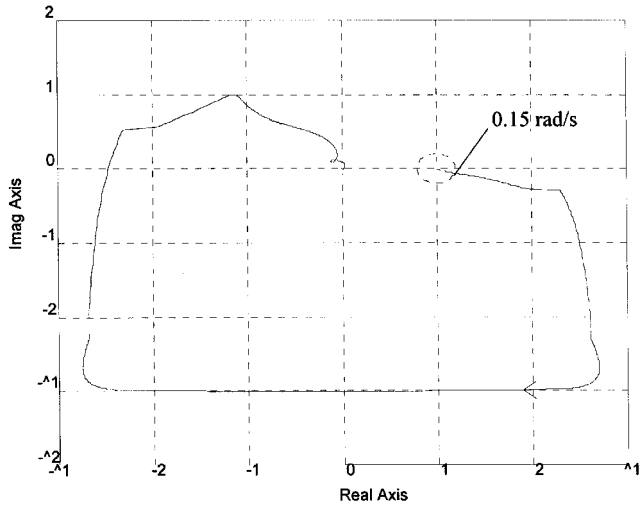

Fig. 6 Nyquist plot of γ_3.

gain and phase margins will only be valid as robustness measures if the MSFs of each channel are sufficiently distant from the (1, 0) point at frequencies of importance.

Figure 6 shows the actual MSF of the $\phi + p$ channel, and it is seen that it is quite close to the (1, 0) point at frequencies below 0.15 rad/s but is adequately far from the (1, 0) point at all other frequencies. The other MSFs were found to be close to the (1, 0) point at frequencies not exceeding 0.15 rad/s and comfortably distant from the (1, 0) point at all other frequencies.

Therefore, there is a possible lack of stability robustness due to loop interaction at low frequency, which could introduce low-frequency unstable modes. Because this possible lack of robustness occurs at frequencies below 0.15 rad/s it is not regarded as being a problem because the pilot is capable of stabilizing low-frequency unstable modes that may develop with a minimal increase in workload.

IX. Handling Qualities Assessment

A. Small-Amplitude Attitude Changes

Figure 7 shows the small amplitude criteria from hover to 80 kn for target acquisition and tracking in low speed and air combat in

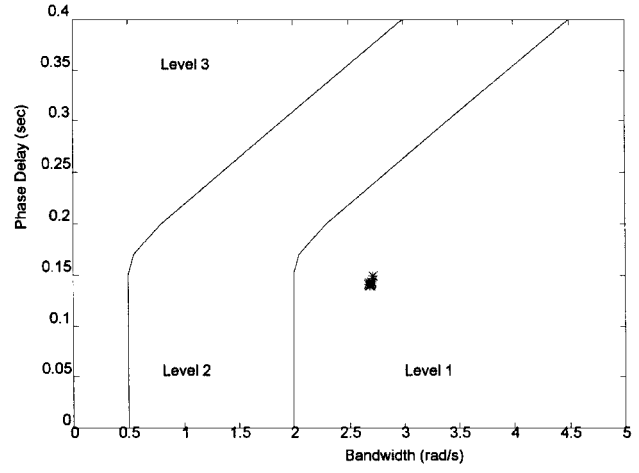

a) Pitch attitude

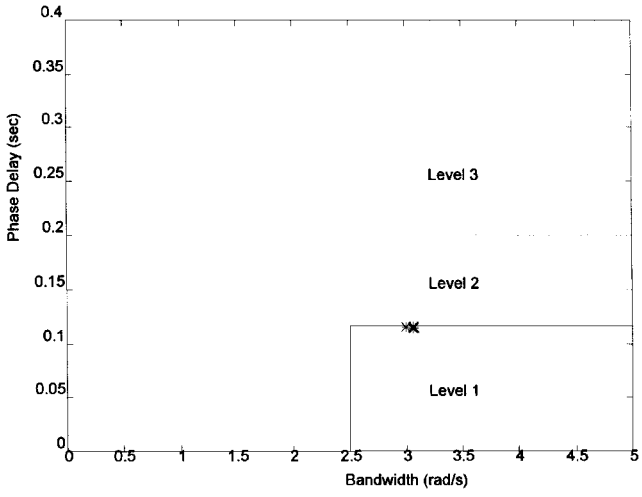

b) Roll attitude

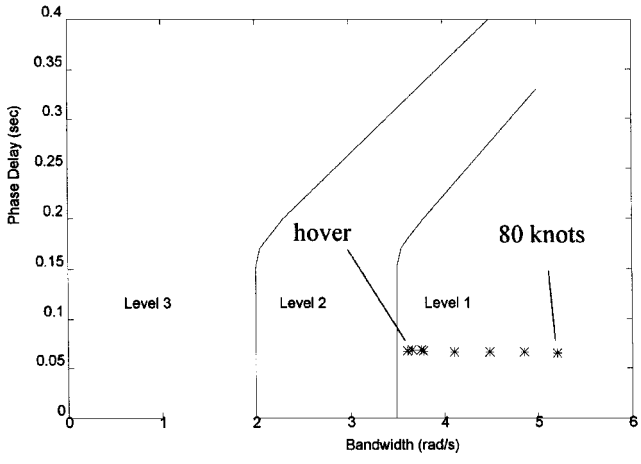

c) Yaw attitude

Fig. 7 Handling qualities bandwidth and phase delay assessment.

forward flight, the most stringent requirements, which share the same boundaries. It is seen that level 1 is met for all three attitude responses over the flight range. Note that, although different linearized helicopter models were computed for each flight condition as necessary using HELISTAB,[11] the controllers were fixed, i.e., there was no gain scheduling.

B. Mid-Term Response

The effective damping factor of the pitch and roll attitude responses was found to be comfortably greater than 0.35 from hover to 80 kn.

Table 7 Height rate response parameters from hover to 40 kn

	$T_{\dot{h}_{eq}}$	$\tau_{\dot{h}_{eq}}$
$\dot{h}/\delta_{coll}$	0.845–1.434	0.124–0.144

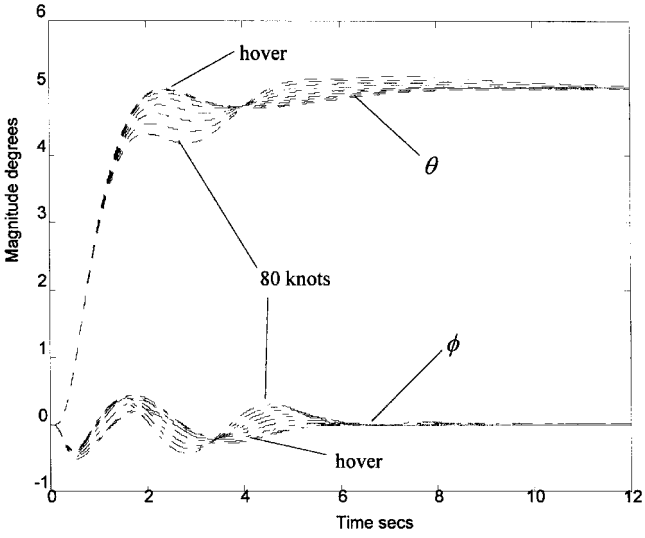

Fig. 8 Pitch and roll attitude response due to a commanded pitch attitude input of 5 deg from hover to 80 kn.

C. Interaxis Coupling

The yaw due to collective coupling was found to meet level 1 requirements from hover to 40 kn. Figure 8 shows the pitch attitude and roll attitude response due to a commanded pitch attitude of 5 deg from hover to 80 kn. It is seen that the coupling is less than 25% and is, hence, level 1. The coupling due to a commanded roll attitude of 5 deg was also found to meet level 1 requirements. In considering Fig. 8, recall that gain scheduling of the controller was not used. The fixed controller was based on the 30-kn flight condition for which the damping is considerably better than that for the hover and 80-kn flight conditions to which the eye is drawn in Fig. 8. A more extensive selection of time responses may be found in Ref. 14.

D. Response to Collective

In hover and low-speed flight, the height rate response is to have a qualitative first-order appearance for the first 5 s following a step input in the collective inceptor. To meet level 1, the equivalent rise time $T_{\dot{h}_{eq}}$ must be less than 5 s and the equivalent time delay $\tau_{\dot{h}_{eq}}$ must be less than 0.2 s. Using a commanded height rate of 5 ft/s, Table 7 shows the spread of $T_{\dot{h}_{eq}}$ and $\tau_{\dot{h}_{eq}}$. It is seen that level 1 requirements are met.

X. Conclusion

This paper has assessed the application of ICAD to the design of a helicopter ACAH system at 30-kn straight and level flight. ICA established that the desired channel bandwidths could be achieved using a diagonal control law and that the design of such a control law would be relatively straightforward, due to the low levels of loop interaction at the desired crossover frequencies. A possible lack of stability robustness due to loop interaction was observed at low frequencies, which could introduce low-frequency unstable modes. Because this lack of robustness occurred below 0.15 rad/s, it was not regarded as being a problem due to the fact that the pilot is capable of stabilizing low-frequency unstable modes with a minimal increase in workload. Although the fixed diagonal control law had only 11 states and the two-element prefilter had only 4 states, the system was found to meet level 1 small-signal requirements from hover to 80 kn, showing that high-order, complex control is not necessary to achieve high performance.

Appendix: Helicopter Model

The following state-space matrices form the 19th-order linear model, produced from HELISTAB,[11] of a typical combat rotorcraft trimmed at 30-kn forward flight:

$$A = \begin{bmatrix} A_{\text{rigidbody}} & \vdots & A_{\text{body/rotor}} & \vdots & \\ \cdots & \cdots & \cdots & \vdots & A_{\text{control}} \\ A_{\text{rotor/body}} & \vdots & A_{\text{rotor}} & \vdots & \\ \cdots & \cdots & \cdots & \cdots & \cdots \\ & 0_A & & \vdots & A_{\text{actuators}} \end{bmatrix}$$

where 0_A is a zero matrix of dimension (4, 15) and

$$A_{\text{rigidbody}} = \begin{bmatrix} 2.056e{-}3 & 3.855e{-}2 & -3.349e{+}0 & -3.212e{+}1 & 1.274e{-}3 & 3.664e{-}2 & 0.000e{+}0 & 0.000e{+}0 & 0.000e{+}0 \\ -1.632e{-}1 & -5.333e{-}1 & 5.122e{+}1 & -2.086e{+}0 & -1.718e{-}2 & -4.941e{-}1 & 1.303e{+}0 & 0.000e{+}0 & 0.000e{+}0 \\ 7.267e{-}4 & -1.137e{-}3 & -1.679e{-}1 & 0.000e{+}0 & 5.269e{-}5 & 1.516e{-}3 & 0.000e{+}0 & 0.000e{+}0 & 0.000e{+}0 \\ 0.000e{+}0 & 0.000e{+}0 & 9.992e{-}1 & 0.000e{+}0 & 0.000e{+}0 & 0.000e{+}0 & 0.000e{+}0 & 4.056e{-}2 & 0.000e{+}0 \\ 1.195e{-}2 & -6.676e{-}4 & 2.112e{-}2 & 8.467e{-}2 & -6.851e{-}2 & 3.191e{+}0 & 3.209e{+}1 & -4.975e{+}1 & 0.000e{+}0 \\ -1.785e{-}3 & -2.689e{-}3 & 3.039e{-}3 & 0.000e{+}0 & 1.707e{-}4 & 1.048e{-}2 & 0.000e{+}0 & -1.203e{-}1 & 0.000e{+}0 \\ 0.000e{+}0 & 0.000e{+}0 & -2.636e{-}3 & 0.000e{+}0 & 0.000e{+}0 & 1.000e{+}0 & 0.000e{+}0 & 6.494e{-}2 & 0.000e{+}0 \\ -1.122e{-}2 & -4.405e{-}3 & -9.598e{-}3 & 0.000e{+}0 & 2.256e{-}2 & 9.593e{-}2 & 0.000e{+}0 & -6.791e{-}1 & 0.000e{+}0 \\ 0.000e{+}0 & 0.000e{+}0 & -4.065e{-}2 & 0.000e{+}0 & 0.000e{+}0 & 0.000e{+}0 & 0.000e{+}0 & 1.001e{+}0 & 0.000e{+}0 \end{bmatrix}$$

$$A_{\text{body/rotor}} = \begin{bmatrix} 0.000e{+}0 & 3.202e{+}1 & 0.000e{+}0 & 0.000e{+}0 & 0.000e{+}0 & 0.000e{+}0 \\ 0.000e{+}0 & 0.000e{+}0 & 0.000e{+}0 & 0.000e{+}0 & 0.000e{+}0 & 0.000e{+}0 \\ 0.000e{+}0 & -2.778e{+}1 & 0.000e{+}0 & 0.000e{+}0 & 0.000e{+}0 & 0.000e{+}0 \\ 0.000e{+}0 & 0.000e{+}0 & 0.000e{+}0 & 0.000e{+}0 & 0.000e{+}0 & 0.000e{+}0 \\ 0.000e{+}0 & 0.000e{+}0 & -3.202e{+}1 & 0.000e{+}0 & 0.000e{+}0 & 0.000e{+}0 \\ 0.000e{+}0 & 7.275e{-}1 & -1.609e{+}2 & 0.000e{+}0 & 0.000e{+}0 & 0.000e{+}0 \\ 0.000e{+}0 & 0.000e{+}0 & 0.000e{+}0 & 0.000e{+}0 & 0.000e{+}0 & 0.000e{+}0 \\ 0.000e{+}0 & 1.615e{+}0 & -2.903e{+}1 & 0.000e{+}0 & 0.000e{+}0 & 0.000e{+}0 \\ 0.000e{+}0 & 0.000e{+}0 & 0.000e{+}0 & 0.000e{+}0 & 0.000e{+}0 & 0.000e{+}0 \end{bmatrix}$$

$$A_{\text{rotor/body}} = \begin{bmatrix} 0.000e+0 & 0.000e+0 & 0.000e+0 & 0.000e+0 & 0.000e+0 & 0.000e+0 & 0.000e+0 & 0.000e+0 & 0.000e+0 \\ 0.000e+0 & 0.000e+0 & 0.000e+0 & 0.000e+0 & 0.000e+0 & 0.000e+0 & 0.000e+0 & 0.000e+0 & 0.000e+0 \\ 0.000e+0 & 0.000e+0 & 0.000e+0 & 0.000e+0 & 0.000e+0 & 0.000e+0 & 0.000e+0 & 0.000e+0 & 0.000e+0 \\ 3.193e-1 & 1.048e+0 & -1.770e+0 & 0.000e+0 & 3.550e-2 & 1.021e+0 & 0.000e+0 & 0.000e+0 & 0.000e+0 \\ -1.536e-1 & -6.815e-1 & 3.264e+1 & 0.000e+0 & 3.644e-1 & 7.264e+1 & 0.000e+0 & 0.000e+0 & 0.000e+0 \\ 3.988e-1 & 1.321e-1 & -7.298e+1 & 0.000e+0 & 5.602e-1 & 3.402e+1 & 0.000e+0 & 0.000e+0 & 0.000e+0 \end{bmatrix}$$

$$A_{\text{rotor}} = \begin{bmatrix} 0.000e+0 & 0.000e+0 & 0.000e+0 & 1.000e+0 & 0.000e+0 & 0.000e+0 \\ 0.000e+0 & 0.000e+0 & 0.000e+0 & 0.000e+0 & 1.000e+0 & 0.000e+0 \\ 0.000e+0 & 0.000e+0 & 0.000e+0 & 0.000e+0 & 0.000e+0 & 1.000e+0 \\ -1.515e+3 & 0.000e+0 & 0.000e+0 & -3.173e+1 & 0.000e+0 & -1.433e+0 \\ -1.021e+2 & -2.453e+2 & -1.131e+3 & 0.000e+0 & -3.173e+1 & -7.126e+1 \\ 0.000e+0 & 1.128e+3 & -2.453e+2 & -2.865e+0 & 7.126e+1 & -3.173e+1 \end{bmatrix}$$

$$A_{\text{actuators}} = \begin{bmatrix} -1.258e+1 & 0.000e+0 & 0.000e+0 & 0.000e+0 \\ 0.000e+0 & -1.258e+1 & 0.000e+0 & 0.000e+0 \\ 0.000e+0 & 0.000e+0 & -1.258e+1 & 0.000e+0 \\ 0.000e+0 & 0.000e+0 & 0.000e+0 & -2.500e+1 \end{bmatrix}$$

$$A_{\text{control}} = \begin{bmatrix} 2.212e+1 & 2.233e+0 & -1.653e-4 & 0.000e+0 \\ -2.983e+2 & -3.011e+1 & 2.315e-3 & 0.000e+0 \\ 9.150e-1 & 9.235e-2 & -6.100e-6 & 0.000e+0 \\ 0.000e+0 & 0.000e+0 & 0.000e+0 & 0.000e+0 \\ -8.572e-1 & -8.635e-2 & 1.033e-5 & 1.5921e+1 \\ 5.664e+0 & 5.715e-1 & 0.000e+0 & -9.705e-1 \\ 0.000e+0 & 0.000e+0 & 0.000e+0 & 0.000e+0 \\ 1.379e+1 & 1.391e+0 & -6.961e-5 & -1.307e+1 \\ 0.000e+0 & 0.000e+0 & 0.000e+0 & 0.000e+0 \\ 0.000e+0 & 0.000e+0 & 0.000e+0 & 0.000e+0 \\ 0.000e+0 & 0.000e+0 & 0.000e+0 & 0.000e+0 \\ 0.000e+0 & 0.000e+0 & 0.000e+0 & 0.000e+0 \\ 7.405e+2 & 6.221e+1 & 0.000e+0 & 0.000e+0 \\ -1.013e+2 & -1.021e+1 & 1.133e+3 & 0.000e+0 \\ 1.640e+2 & 1.134e+3 & 0.000e+0 & 0.000e+0 \end{bmatrix}, \qquad B = \begin{bmatrix} & & 0_B & \\ \cdots & \cdots & \cdots & \cdots \\ 1.258e+1 & 0.000e+0 & 0.000e+0 & 0.000e+0 \\ 0.000e+0 & 1.258e+1 & 0.000e+0 & 0.000e+0 \\ 0.000e+0 & 0.000e+0 & 1.258e+1 & 0.000e+0 \\ 0.000e+0 & 0.000e+0 & 0.000e+0 & 2.500e+1 \end{bmatrix}$$

$$C = \begin{bmatrix} 1.297e-2 & -1.994e-1 & 0.000e+0 & 1.013e+1 & 8.095e-3 & 0.000e+0 & -2.662e-2 & 0.000e+0 & \vdots & \\ 0.000e+0 & 0.000e+0 & 1.146e+1 & 1.146e+1 & 0.000e+0 & 0.000e+0 & 0.000e+0 & 0.000e+0 & \vdots & 0_C \\ 0.000e+0 & 0.000e+0 & 0.000e+0 & 0.000e+0 & 0.000e+0 & 1.146e+1 & 1.146e+1 & 0.000e+0 & \vdots & \\ 0.000e+0 & 0.000e+0 & 0.000e+0 & 0.000e+0 & 0.000e+0 & 0.000e+0 & 0.000e+0 & 1.146e+1 & \vdots & \end{bmatrix}$$

where 0_B is a zero matrix of dimension (15, 4) and 0_C is a zero matrix of dimension (4, 11).

The state vector is

$$\boldsymbol{x} = \begin{bmatrix} u & w & q & \theta & v & p & \phi & r & \psi & \beta_0 & \beta_{1c} & \beta_{1s} & \dot{\beta}_0 & \dot{\beta}_{1c} & \dot{\beta}_{1s} & \theta_{0_{\text{act}}} & \theta_{1s_{\text{act}}} & \theta_{1c_{\text{act}}} & \theta_{0T_{\text{act}}} \end{bmatrix}$$

Acknowledgment

The authors wish to thank the Defence Evaluation and Research Agency (Bedford) for supplying HELISTAB and the Handling Qualities Toolbox.

References

[1]Directorate for Engineering, "Aeronautical Design Standard—Handling Qualities Requirements for Military Rotorcraft (ADS-33D)," U.S. Army Aviation and Troop Command, St. Louis, MO, July 1994.

[2]Low, E., and Garrard, W. L., "Design of Flight Control Systems to Meet Rotorcraft Handling Qualities Specifications," *Journal of Guidance, Control, and Dynamics*, Vol. 16, No. 1, 1993, pp. 69–78.

[3]Manness, M. A., and Murray-Smith, D. J., "Aspects of Multivariable Flight Control Law Design for Helicopters Using Eigenstructure Assignment," *Journal of the American Helicopter Society*, Vol. 37, No. 3, 1992, pp. 18–32.

[4]Takahashi, M. D., "H_∞ Helicopter Flight Control Law Design With and Without Rotor State Feedback," *Journal of Guidance, Control, and Dynamics*, Vol. 17, No. 6, 1994, pp. 1245–1251.

[5]Walker, D. J., and Postlethwaite, I., "Advanced Helicopter Flight Control Using Two-Degree-Of-Freedom H Optimization," *Journal of Guidance, Control, and Dynamics*, Vol. 19, No. 2, 1996, pp. 461–468.

[6]Gribble, J. J., "Linear Quadratic Gaussian/Loop Transfer Recovery Design for a Helicopter in Low Speed Flight," *Journal of Guidance, Control, and Dynamics*, Vol. 16, No. 4, 1993, pp. 754–761.

[7]Dudgeon, G. J. W., "Individual Channel Analysis and Design and Its Application to Helicopter Flight Control," Ph.D. Thesis, Dept. of Electronics and Electrical Engineering, Univ. of Glasgow, Glasgow, Scotland, UK, Oct. 1996.

[8]Leithead, W. E., and O'Reilly, J., "M-Input M-Output Feedback-Control by Individual Channel Design. Part 1., Structural Issues," *International Journal of Control*, Vol. 56, No. 6, 1992, pp. 1347–1397.

[9]Leithead, W. E., and O'Reilly, J., "Investigation of the ICD Structure of Systems Defined by State-Space Models," *International Journal of Control*, Vol. 60, No. 1, 1994, pp. 71–89.

[10]Liceaga-Castro, J., Verde, C., O'Reilly, J., and Leithead, W. E., "Helicopter Flight Control Using Individual Channel Design," *IEE Proceedings—Control Theory and Applications*, Vol. 142, No. 1, 1995, pp. 58–72.

[11]Smith, J., "An Analysis of Helicopter Flight Mechanics Part 1—Users Guide to the Software Package HELISTAB," Royal Aircraft Establishment, TM FS(B) 569, Bedford, England, UK, Oct. 1984.

[12]Tischler, M. B., "Digital Control of Highly Augmented Combat Rotorcraft, NASA TM 88346, USAAVSCOM TR 87-A-5, May 1987.

[13]Mayne, D. Q., "The Design of Linear Multivariable Systems," *Automatica*, Vol. 9, No. 2, 1973, pp. 201–207.

[14]Dudgeon, G. J. W., Gribble, J. J., and O'Reilly, J., "Individual Channel Analysis and Helicopter Flight Control in Moderate- and Large-Amplitude Manoeuvres," *Control Engineering Practice*, Vol. 5, No. 1, 1997, pp. 33–38.